

Regulation of apical NHE3 trafficking by ouabain-induced activation of the basolateral Na⁺-K⁺-ATPase receptor complex

Haiping Cai, Liang Wu, Weikai Qu, Deepak Malhotra, Zijian Xie, Joseph I. Shapiro and Jiang Liu

Am J Physiol Cell Physiol 294:555-563, 2008. First published Dec 12, 2007;
doi:10.1152/ajpcell.00475.2007

You might find this additional information useful...

This article cites 56 articles, 37 of which you can access free at:

<http://ajpcell.physiology.org/cgi/content/full/294/2/C555#BIBL>

Updated information and services including high-resolution figures, can be found at:

<http://ajpcell.physiology.org/cgi/content/full/294/2/C555>

Additional material and information about *AJP - Cell Physiology* can be found at:

<http://www.the-aps.org/publications/ajpcell>

This information is current as of June 24, 2008 .

Regulation of apical NHE3 trafficking by ouabain-induced activation of the basolateral Na⁺-K⁺-ATPase receptor complex

Haiping Cai,^{1*} Liang Wu,^{1*} Weikai Qu,¹ Deepak Malhotra,¹ Zijian Xie,^{1,2} Joseph I. Shapiro,^{1,2} and Jiang Liu¹

Departments of ¹Medicine and ²Pharmacology, University of Toledo College of Medicine, Toledo, Ohio

Submitted 10 October 2007; accepted in final form 6 December 2007

Cai H, Wu L, Qu W, Malhotra D, Xie Z, Shapiro JI, Liu J. Regulation of apical NHE3 trafficking by ouabain-induced activation of the basolateral Na⁺-K⁺-ATPase receptor complex. *Am J Physiol Cell Physiol* 294: C555–C563, 2008; doi:10.1152/ajpcell.00475.2007.—The long-term effects of ouabain on transepithelial Na⁺ transport involve transcriptional downregulation of apical Na⁺/H⁺ exchanger isoform 3 (NHE3). The aim of this study was to determine whether ouabain could acutely regulate NHE3 via a posttranscriptional mechanism in LLC-PK1 cells. We observed that the basolateral, but not apical, application of ouabain for 1 h significantly reduced transepithelial Na⁺ transport. This effect was not due to changes in the integrity of tight junctions or increases in the intracellular Na⁺ concentration. Ouabain regulated the trafficking of NHE3 and subsequently inhibited its activity, a process independent of intracellular Na⁺ concentration. Ouabain-induced NHE3 trafficking was abolished by either cholesterol depletion or Src inhibition. Moreover, ouabain increased the intracellular Ca²⁺ concentration. Pretreatment of cells with the intracellular Ca²⁺ chelator BAPTA-AM blocked ouabain-induced trafficking of NHE3. Also, blockade of Na⁺-K⁺-ATPase endocytosis by a phosphatidylinositol 3-kinase inhibitor was equally effective in attenuating ouabain-induced NHE3 trafficking. These data indicate that ouabain acutely stimulates NHE3 trafficking by activating the basolateral Na⁺-K⁺-ATPase signaling complex. Taken together with our previous observations, we propose that ouabain can simultaneously regulate basolateral Na⁺-K⁺-ATPase and apical NHE3, leading to inhibition of transepithelial Na⁺ transport. This mechanism may be relevant to proximal tubular Na⁺ handling during conditions associated with increases in circulating endogenous cardiotoxic steroids.

kidney; sodium; sodium/hydrogen exchanger isoform 3; trafficking; c-Src; phosphatidylinositol 3-kinase

SODIUM/HYDROGEN EXCHANGERS (NHEs) are present in all mammalian cells. They are involved in regulating intracellular pH, cellular volume, and cell growth. In the renal proximal tubule, NHE3 and Na⁺-K⁺-ATPase are critical in transepithelial Na⁺ reabsorption. We have previously reported that in LLC-PK1 cells (a widely accepted pig renal proximal tubule cell line), exposure to low concentrations of ouabain (≤100 nM) for 12–24 h not only causes significant depletion of basolateral Na⁺-K⁺-ATPase but also induces downregulation of NHE3 expression and activity. These regulations are dependent on the ouabain-activated signaling function of Na⁺-K⁺-ATPase, and they cause substantial inhibition of transepithelial ²²Na⁺ transport without affecting the intracellular Na⁺ concentration ([Na⁺]_i) (33, 43).

* H. Cai and L. Wu contributed equally to this work.

Address for reprint requests and other correspondence: J. Liu, Dept. of Medicine, Univ. of Toledo College of Medicine, 3120 Glendale Ave., Toledo, OH 43614-5089 (e-mail: jiang.liu@utoledo.edu).

Endogenous cardiotoxic steroids, including ouabain and marinobufagenin, are now accepted as a new class of steroid hormones that are involved in blood pressure regulation and renal Na⁺ handling (18, 19, 23, 26, 46). Elevated endogenous ouabain levels have been found in a number of clinical conditions that are associated with plasma volume expansion such as chronic renal failure, hypertension, and congestive heart failure. The cardiotoxic steroid binding site of Na⁺-K⁺-ATPase is believed to be the same molecular target of the hypertensive effects of these compounds, and this binding site appears to play an important role in blood pressure regulation (18).

Na⁺ reabsorption in the proximal tubule involves the coupling of apical Na⁺ entry via NHE3 and other transporters, whereas basolateral Na⁺ extrusion occurs primarily through Na⁺-K⁺-ATPase. Our previous observations have suggested that the effects of endogenous cardiotoxic steroids on NHE3 may represent an adaptive response to volume expansion, a concept that resonates with early theories proposing the existence of one or more endogenous natriuretic compounds, as introduced by Dahl et al. (13), Blaustein (8), and de Wardener and Clarkson EM (14). It seems logical to propose that synchronous regulation of Na⁺-K⁺-ATPase and NHE3 may present a functional loop that regulates coordinated transepithelial Na⁺ transport in this nephron segment.

NHE3 activity is controlled by phosphorylation, trafficking, and transcriptional regulation. Regulated NHE3 trafficking has been demonstrated in many cases that involve clathrin- and/or lipid raft-dependent pathways (10, 31). Although the specific mechanisms through which cardiotoxic steroids affect NHE3-mediated renal Na⁺ handling are still being elucidated, evidence supports the notion that endogenous cardiotoxic steroids might cause a physiologically meaningful regulation of transepithelial Na⁺ transport in the renal proximal tubule. NHE3 has been shown to be redistributed in hypertension, accompanying reversible downregulation of Na⁺-K⁺-ATPase activity in the renal cortex (56). In opossum kidney cells, overexpression of the Na⁺-K⁺-ATPase α₁-subunit upregulated apical NHE3 activity and abundance, resulting in the stimulation of apical Na⁺ influx (20). Parathyroid hormone and dopamine have been shown to stimulate endocytosis of Na⁺-K⁺-ATPase and NHE3 (9, 11, 25, 27). Salt loading in vivo not only significantly depressed NHE3 expression but also induced Na⁺-K⁺-ATPase endocytosis in a marinobufagenin-dependent manner (3, 44).

We have recently reported the mechanism through which ouabain-induced transcriptional downregulation of NHE3 oc-

The costs of publication of this article were defrayed in part by the payment of page charges. The article must therefore be hereby marked “advertisement” in accordance with 18 U.S.C. Section 1734 solely to indicate this fact.

curs. This results in decreased transepithelial Na^+ transport. Since we have shown that the activation of the basolateral $\text{Na}^+-\text{K}^+-\text{ATPase}/\text{Src}$ receptor complex by ouabain stimulated endocytosis of $\text{Na}^+-\text{K}^+-\text{ATPase}$, we reasoned that this might also regulate NHE3 trafficking so that apical NHE3 activity can be coupled to the basolateral $\text{Na}^+-\text{K}^+-\text{ATPase}$ activity to keep intracellular Na^+ homeostasis. To test this hypothesis, the following experiments were conducted.

MATERIALS AND METHODS

Materials and cell culture. All chemicals, except otherwise mentioned, were obtained from Sigma (St. Louis, MO). Wortmannin, protein phosphatase 2 (PP2), and 1,2 bis(2-aminophenoxy)ethane-*N,N,N',N'*-tetra-acetic acid-acetoxymethyl ester (BAPTA-AM) were obtained from Calbiochem (San Diego, CA). $^{22}\text{Na}^+$ was obtained from DuPont NEN Life Science (Boston, MA).

A rabbit polyclonal antibody against a mixture of peptides from porcine NHE3 was prepared and affinity purified (43). Horseradish peroxidase-conjugated goat anti-rabbit IgG and antibodies against early endosome antigen-1 (EEA1), Rab5, and Rab7 were obtained from Santa Cruz Biotechnology (Santa Cruz, CA). Polyclonal antibodies against occludin and claudin-1 were obtained from Zymed Laboratories (San Francisco, CA). A monoclonal antibody against the $\text{Na}^+-\text{K}^+-\text{ATPase}$ α_1 -subunit (clone $\alpha 6\text{F}$) was obtained from the Hybridoma Bank of the University of Iowa (Iowa City, IA).

The LLC-PK1 cell line was obtained from the American Type Culture Collection (Manassas, VA) and cultured in DMEM containing 10% FBS, penicillin (100 U/ml), and streptomycin (100 $\mu\text{g}/\text{ml}$) in a 5% CO_2 -humidified incubator. All cells were serum starved for 12 h before experiments.

Measurements of intracellular Na^+ and Ca^{2+} concentrations. $[\text{Na}^+]_i$ and intracellular Ca^{2+} concentration ($[\text{Ca}^{2+}]_i$) were measured using a computer-controlled spectrophotometer (PTI, London, ON, Canada) with Felix software (PTI) as previously described (36, 43). Perfusion was set at a rate of 1 ml/min with a corresponding physiological salt solution. For $[\text{Na}^+]_i$ measurements, LLC-PK1 cells were loaded with 10 μM of the Na^+ -sensitive fluorescent dye SBFI-AM (Molecular Probes, Eugene, OR) in the presence of 0.2% pluronic F-127 (Molecular Probes) in physiological salt buffer [containing (in mM) 110 NaCl, 3 KCl, 10 HEPES, 5 D-glucose, 1 CaCl_2 , 1.2 MgSO_4 , 1 NaHCO_3 , and 1 KH_2PO_4 , with pH7.4 adjusted with Tris]. Fluorescent emissions were monitored at 510 nm to obtain excitation ratios (F_{340}/F_{380}) by dual excitations at 340/380 nm. Calibration was performed in situ with known concentrations of Na^+ in the presence of 5 μM of Na^+ ionophore gramicidin and 10 μM monensin (17). For $[\text{Ca}^{2+}]_i$ measurements, LLC-PK1 cells were loaded with 2 μM of the Ca^{2+} -sensitive fluorescent dye fura-2-AM (Molecular Probes) in physiological salt buffer [containing (in mM) 100 NaCl, 4 KCl, 20 HEPES, 10 D-glucose, 1 CaCl_2 , 1.2 MgCl_2 , 25 NaHCO_3 , and 1 NaH_2PO_4 ; pH7.4], and fura-2 fluorescent emissions were monitored at 510 nm to obtain excitation ratios (F_{340}/F_{380}) by dual excitations at 340/380 nm. $[\text{Ca}^{2+}]_i$ was calculated based on the fluorescence ratio and the in situ Ca^{2+} calibration using Ca^{2+} ionophore ionomycin and the extracellular Ca^{2+} chelating agent EGTA.

NHE3 activity and active transepithelial $^{22}\text{Na}^+$ transport. The intracellular pH recovery rate and $^{22}\text{Na}^+$ uptake were determined as previously described (43). Calibration of intracellular pH was performed using high- K^+ -nigericin (10 μM) standards (41). During measurements of intracellular pH and $^{22}\text{Na}^+$ uptake, 50 μM amiloride was used to inhibit amiloride-sensitive NHE1 activity. To measure active transepithelial $^{22}\text{Na}^+$ flux, a transepithelial $^{22}\text{Na}^+$ transport assay was performed in LLC-PK1 monolayers (grown on Costar Transwell culture filter inserts, filter pore size: 0.4 μm , Costar, Cambridge, MA). LLC-PK1 monolayers were first treated with or without ouabain (100 nM) applied in the basolateral or apical com-

partment, and active transepithelial $^{22}\text{Na}^+$ flux (apical to basolateral) was determined by counting radioactivity in the basolateral aspect at 1 h after $^{22}\text{Na}^+$ addition.

Western blot analysis. Whole cell lysates were prepared using ice-cold RIPA buffer [containing 1% Nonidet P-40, 0.25% sodium deoxycholate, 150 mM NaCl, 50 mM Tris·HCl (pH 7.4), 1 mM EDTA, 1 mM PMSF, 1 mM sodium orthovanadate, 1 mM NaF, 10 $\mu\text{g}/\text{ml}$ aprotinin, and 10 $\mu\text{g}/\text{ml}$ leupeptin]. Cell lysates were then centrifuged (4°C, 16,000 g, 10 min), and equal amounts of total protein from the supernatants were used for Western blot analysis. The membrane fraction was isolated as previously described (15) using nondetergent membrane buffer (same as RIPA buffer but without Nonidet P-40 and sodium deoxycholate). Cells were collected, homogenized, and microfuged (4°C, 16,000 g, 10 min) to remove insoluble cell debris and unbroken cells. Supernatants were further centrifuged (109,000 g at the maximum radius for 30 min at 4°C), and pellets were resuspended in 1× Laemmli sample buffer. For the Western blot analysis, equal amounts of total protein were resolved by 10% SDS-PAGE and immunoblotted with antibodies against NHE3, the $\text{Na}^+-\text{K}^+-\text{ATPase}$ α_1 -subunit, occludin, or claudin-1. The same membrane was stripped and immunoblotted with anti-tubulin antibody to serve as an internal loading control. Signal detection was performed with an enhanced chemiluminescence super signal kit (Pierce, Rockford, IL). Multiple exposures were analyzed to assure that the signals were within the linear range of the film. The signal density was determined using Molecular Analyst software (Bio-Rad, Hercules, CA).

Labeling of cell surface proteins by biotinylation. Cell surface protein biotinylation was performed as previously described (22, 33). LLC-PK1 cells were grown to form monolayers (6–7 days) on 24-mm polycarbonate Transwell culture filter inserts (filter pore size: 0.4 μm , Costar). The culture medium was replaced daily until 12 h before experiments, at which point the monolayer was serum starved. After surface biotinylation with EZ-Link sulfo-NHS-ss-Biotin (Pierce) and immobilization with ImmunoPure immobilized streptavidin-agarose beads (Pierce), biotinylated proteins were eluted by an incubation in a 55°C water bath for 30 min with an equal volume of 2× Laemmli sample buffer, resolved by 10% SDS-PAGE, and then immunoblotted.

Isolation of early and late endosomes. Early and late endosomes were fractionated on a flotation gradient using the technique of Gorvel et al. (21). Early and late endosome fractions were identified with antibodies against EEA1 and Rab5 (early endosome marker proteins) as well as Rab7 (late endosome marker protein). The method has been verified as we have previously described (33). For each sample or treatment, LLC-PK1 cells were grown on three 150-mm dishes and subjected to endosomal isolation.

Cholesterol depletion and repletion. Methyl- β -cyclodextrin (M β -CD; Sigma) was dissolved in DMEM and used directly as previously described (50). Cholesterol depletion was carried out by incubating the cells in the presence of 10 mM M β -CD for 30 min at 37°C. Cells were washed twice with serum-free medium before experiments. Cholesterol repletion was carried out by incubating cholesterol-depleted cells with DMEM containing 4% (vol/vol) cholesterol-M β -CD stock solution for 1 h at 37°C. Cholesterol-M β -CD stock solution was prepared by mixing 200 μl of cholesterol (20 mg/ml in ethanol) with 10 ml of 10% M β -CD solution by vortexing at 40°C.

Immunofluorescence microscopy. Immunofluorescence and confocal microscopy were performed as previously described (33). LLC-PK1 monolayers grown on Transwell filters were fixed in chilled (−20°C) methanol (100%), permeabilized for 15 min with permeabilization buffer (0.3% Triton X-100 and 0.1% BSA in PBS with 0.1 mM CaCl_2 and 1 mM MgCl_2), and blocked for 30 min with blocking buffer [containing 150 mM NaCl and 20 mM sodium phosphate (pH7.4) with 0.3% Triton X-100 and 16% (vol/vol) normal goat or horse serum]. Cells were incubated with primary antibodies (anti-occludin or anti-claudin-1, 1:50 in blocking buffer) overnight at 4°C

and washed three times with permeabilization buffer. Cells were then incubated with Alexa fluor 488-conjugated secondary antibody (1:100 in blocking buffer, Molecular Probes) for 1 h at room temperature, washed three times with permeabilization buffer, mounted in Prolong Antifade mounting medium (Molecular Probes), and dried in the dark overnight at room temperature. Confocal images were captured by a Leica TCS SP2 spectral confocal scanner and a Leica DMIRE2 microscope (Leica, Mannheim, Germany) equipped with a $\times 63$ oil-immersion objective. Visualization and analysis were performed using Leica confocal microscope system software.

Statistical analysis. Data were tested for normality (all data passed) and then subjected to parametric analysis. When more than two groups were compared, one-way ANOVA was performed prior to comparison of individual groups with an unpaired t-test. Bonferroni's correction for multiple comparisons was employed as appropriate. Statistical significance was reported at the $P < 0.05$ and $P < 0.01$ levels. SPSS software was used for all analysis (SPSS, Chicago, IL).

RESULTS

Ouabain induces inhibition of NHE3 activity in LLC-PK1 cells. We have shown that ouabain stimulates endocytosis of basolateral $\text{Na}^+\text{-K}^+\text{-ATPase}$ in LLC-PK1 cells (33). Over 12–24 h, ouabain reduced NHE3 mRNA and protein expression (43), leading to significantly reduced transepithelial Na^+ transport in LLC-PK1 monolayers without altering $[\text{Na}^+]_i$. Since 100 nM ouabain failed to increase intracellular Na^+ , a balance of Na^+ influx and efflux was expected. We assessed the acute effect of low concentrations of ouabain on NHE3 activity by measuring Na^+ -dependent intracellular pH recovery and H^+ -driven $^{22}\text{Na}^+$ uptake. For these measurements, LLC-PK1 cells were grown to confluence on glass coverslips or 12-well plates, serum starved for 12 h, and then treated with or without ouabain (100 nM) for different intervals. These assays were performed in the presence of 50 μM amiloride to inhibit NHE1 activity. To determine H^+ -driven Na^+ uptake, cells were first acid loaded in Na^+ -free buffer with 20 mM NH_4Cl and then assayed for $^{22}\text{Na}^+$ uptake. Ouabain (100 nM) treatment significantly decreased H^+ -driven $^{22}\text{Na}^+$ uptake in a time-dependent manner (Fig. 1A). To determine if ouabain-induced decreases in $^{22}\text{Na}^+$ uptake were due to the inhibition of NHE3 activity, the Na^+ -stimulated pH recovery rate after Na^+ reintroduction was also determined. After ouabain treatment (100 nM, 1 h), the Na^+ -stimulated pH recovery rate was also decreased by $\sim 30\%$ (0.22 ± 0.04 pH units/min, $n = 8$) compared with control cells (0.32 ± 0.05 pH units/min, $n = 8$, $P < 0.01$; Fig. 1B). To evaluate the acute ouabain effect on transepithelial Na^+ transport, LLC-PK1 cells were grown on Transwell filters to form monolayers. Ouabain (100 nM, 1 h) was applied to the basolateral or apical aspect, and transepi-

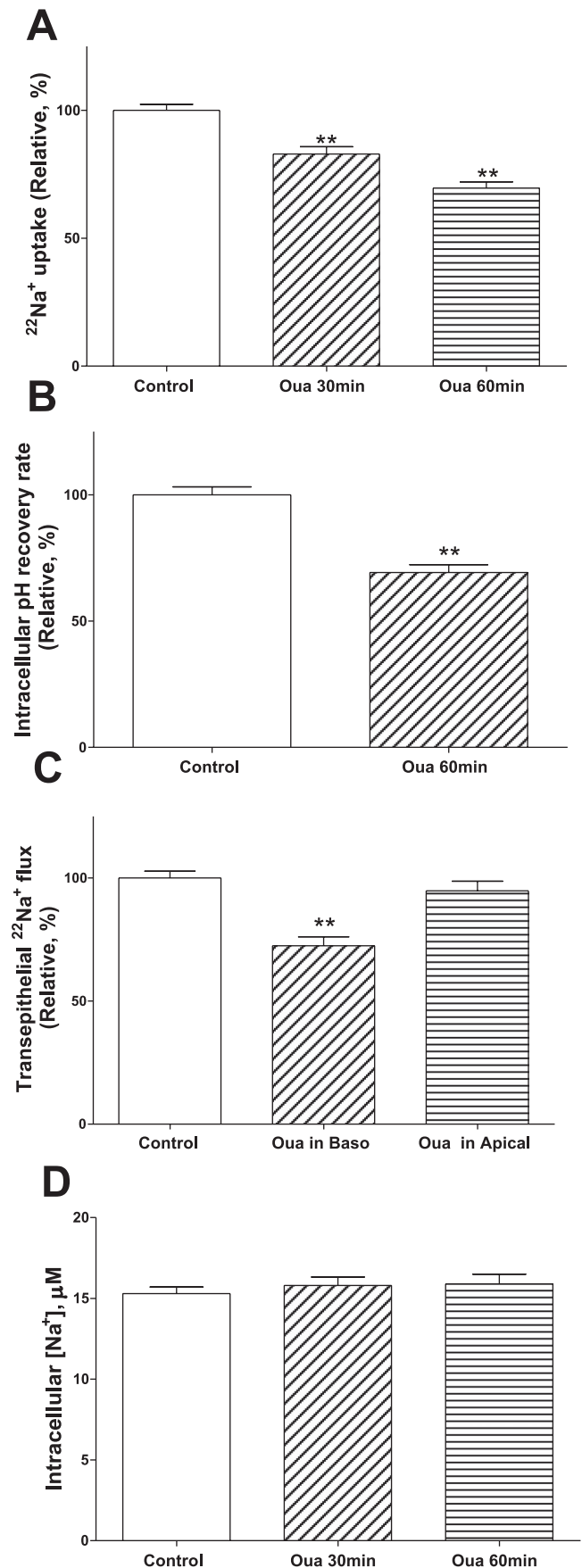


Fig. 1. Ouabain (Oua) inhibits Na^+/H^+ exchanger isoform 3 (NHE3) activity and transepithelial $^{22}\text{Na}^+$ transport. LLC-PK1 cells were treated with or without 100 nM ouabain for the indicated times. H^+ -driven $^{22}\text{Na}^+$ uptake, Na^+ -dependent intracellular pH recovery, transepithelial $^{22}\text{Na}^+$ transport, and intracellular Na^+ concentration ($[\text{Na}^+]_i$) were measured as described in MATERIALS AND METHODS. A: H^+ -driven $^{22}\text{Na}^+$ uptake after ouabain (100 nM) treatment ($n = 6$). B: Na^+ -dependent intracellular pH recovery after ouabain (100 nM, 1 h) treatment ($n = 8$). C: effects of ouabain (100 nM, 1 h) treatment on transepithelial $^{22}\text{Na}^+$ transport ($n = 6$). Ouabain was applied to the basolateral (Baso) or apical aspect of LLC-PK1 monolayers grown on Transwell filter supports. D: effects of ouabain (100 nM) treatment on $[\text{Na}^+]_i$ ($n = 12$). For bar graphs, values are means \pm SE and are expressed relative to the control. $**P < 0.01$, ouabain treatment vs. control.

thelial $^{22}\text{Na}^+$ flux (from apical to basolateral compartments) was determined. Ouabain treatment in the basolateral aspect significantly reduced transepithelial $^{22}\text{Na}^+$ flux, but no such effect was observed with apical exposure to ouabain ($n = 6$; Fig. 1C). Since high concentrations of ouabain have been shown to increase $[\text{Na}^+]_i$, depolarize proximal tubule cells, and affect the tight junction integrity of epithelial cells (6, 42, 45), we further evaluated if low concentrations of ouabain have any acute effects on $[\text{Na}^+]_i$ and tight junctions. In LLC-PK1 cells, real-time $[\text{Na}^+]_i$ measurements did not show any significant $[\text{Na}^+]_i$ change in response to ouabain (100 nM; Fig. 1D). However, $[\text{Na}^+]_i$ was significantly increased in response to high concentrations of ouabain (10 and 100 μM , 30 min; data not shown). In LLC-PK1 monolayers, a low concentration of ouabain (100 nM) did not show any effect on transepithelial electrical resistance (45). Consistently, low concentrations of ouabain have no discernable effects on tight junctions. Ouabain (100 nM for 1 h and up to 6 h) did not alter the expression (Fig. 2A) or distribution of two tight junction proteins, occludin (Fig. 2, B and C) and claudin-1 (data not shown). In contrast, when LLC-PK1 monolayers were washed and incubated in Ca^{2+} -free (with 1 mM EDTA) medium for 5 min before being immunostained for occludin, some broken tight junctions (defined as loss of tight contact of plasma membrane between two adjacent cells) could be demonstrated (Fig. 2D).

The present data are consistent with the notion that ouabain-induced inhibition of NHE3 activity is due to the effect(s) of ouabain on basolateral $\text{Na}^+-\text{K}^+-\text{ATPase}$, which regulates both ion transporters to maintain intracellular Na^+ homeostasis.

Ouabain-induced NHE3 trafficking leads to the inhibition of NHE3 activity in LLC-PK1 cells. The observed acute change in NHE3 activity is most likely due to an alteration in NHE3 trafficking, because ouabain had no acute effect on NHE3 mRNA or total NHE3 protein expression up to 6 h (data not shown). To determine if ouabain could regulate NHE3 trafficking, we examined the distribution of NHE3 on the cell surface and in endosomes in response to ouabain.

After LLC-PK1 cells were treated with or without ouabain (100 nM, 1 h), whole cell lysates and membrane fractions were prepared and analyzed by Western blot. Tubulin served as the loading control. As shown in Fig. 3, whereas chronic ouabain treatment (100 nM, 12 h) significantly reduced NHE3 expression in whole cell lysates (43), acute ouabain treatment (100 nM, 1 h) had no effect on NHE3 protein content in whole cell lysates ($P > 0.05$, $n = 6$; Fig. 3A), but it significantly reduced NHE3 content in membrane fractions ($P < 0.01$, $n = 6$; Fig. 3B). These observations were further confirmed by cell surface biotinylation experiments, which showed a significant decrease in cell surface NHE3 protein content in response to ouabain (100 nM, 1 h) added to the basolateral but not apical compartment ($P < 0.01$, $n = 4$; Fig. 3C). The observed decrease in NHE3 protein abundance in cell surface and membrane fractions, but not in whole cell lysates, suggests a redistribution of NHE3 in response to acute ouabain treatment. Under these conditions, the $\text{Na}^+-\text{K}^+-\text{ATPase}$ α_1 -subunit was also redistributed in the same pattern as seen in NHE3 (data not shown), consistent with our early observation (33).

In addition to cell surface biotinylation, early and late endosomes were isolated to explore the redistribution status of NHE3. Early and late endosomes were isolated and identified with anti-EEA1, Rab5, and Rab7 antibodies. Ouabain (100 nM,

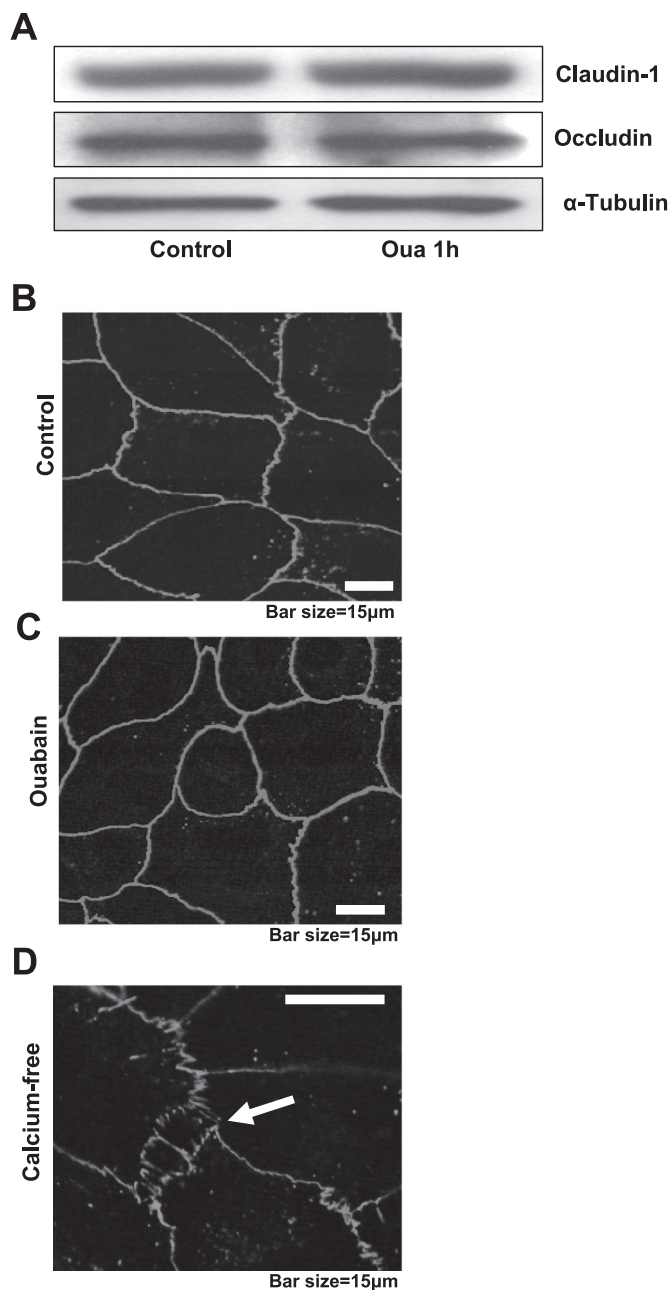


Fig. 2. Ouabain has no significant effect on the integrity of tight junctions in LLC-PK1 monolayers. LLC-PK1 monolayers were treated with or without 100 nM ouabain for 1 h. The abundance of occludin and claudin-1 in whole cell lysates were measured by Western blot analysis; tubulin served as a loading control. Occludin distribution was imaged with confocal microscopy after fluorescence immunostaining. A: representative Western blot showing the abundance of occludin and claudin-1 in whole cell lysates. No significant differences were observed ($P > 0.05$, ouabain vs. control; $n = 3$). B–D: distribution of occludin in LLC-PK1 monolayers under control conditions (B), with ouabain treatment (C), and after preincubated in Ca^{2+} -free medium for 5 min (D). The arrow shows a disrupted tight junction. Bars = 15 μm .

1 h) treatment significantly accumulated NHE3 protein in early endosomes ($P < 0.01$, $n = 9$; Fig. 4). Interestingly, the $\text{Na}^+-\text{K}^+-\text{ATPase}$ α_1 -subunit was also accumulated and coexisted with NHE3 in the same early endosome preparation in response to ouabain ($P < 0.01$, $n = 9$; Fig. 4). It is important to note that the accumulation of both proteins in the early

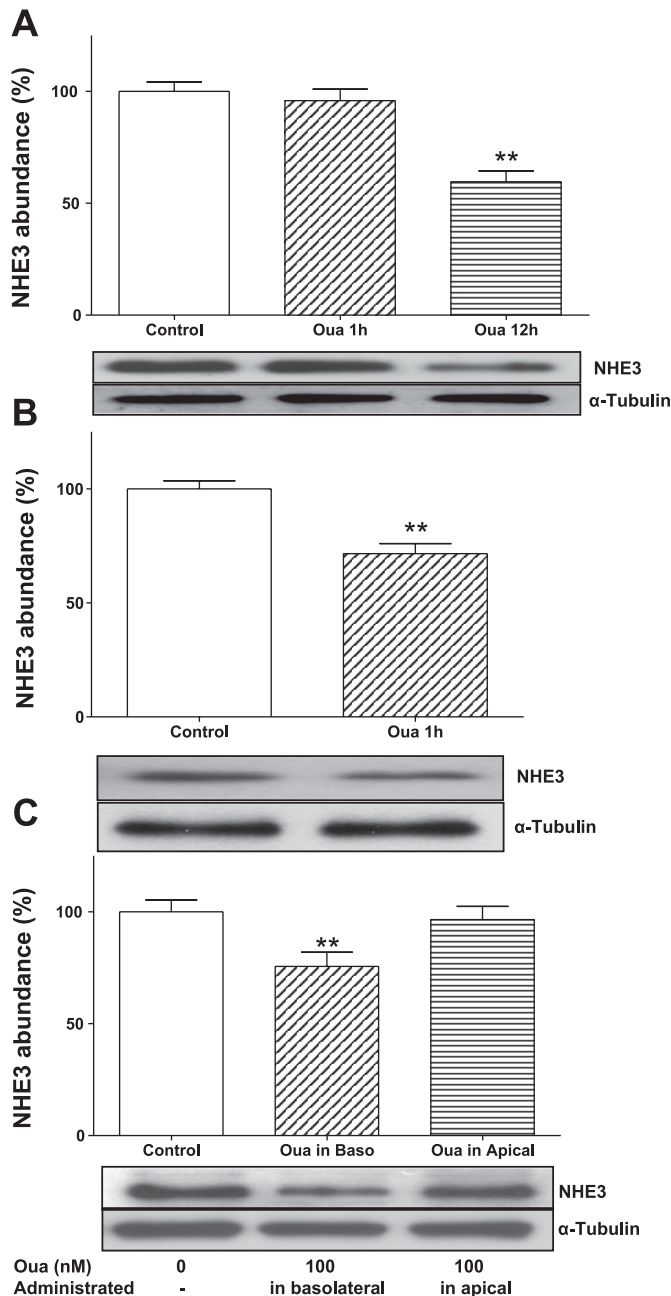


Fig. 3. Ouabain causes NHE3 redistribution in LLC-PK1 cells. **A**: representative Western blot of whole cell lysates before and after ouabain treatment (100 nM; *bottom*) and bar graph summary of the immunoblotting data ($n = 6$; *top*). **B**: representative Western blot of membrane-associated NHE3 protein abundance before and after ouabain treatment (100 nM, 1 h; *bottom*) and bar graph summary of the immunoblotting data ($n = 6$; *top*). **C**: representative Western blot of cell surface NHE3 as detected by cell surface protein biotinylation before and after ouabain treatment (100 nM, 1 h; *bottom*) and bar graph summary of the immunoblotting data ($n = 4$; *top*). For bar graphs, values are means \pm SE and are expressed relative to the control. ** $P < 0.01$, ouabain treatment vs. control.

endosomes appears to occur simultaneously, indicating coordinated regulation of both ion transporters by ouabain. Under these conditions, the $\text{Na}^+\text{-K}^+\text{-ATPase}$ α_1 -subunit was also accumulated in late endosomes, but no detectable NHE3 protein was observed in late endosomes (data not shown).

Activation of the basolateral $\text{Na}^+\text{-K}^+\text{-ATPase}/\text{Src}$ receptor complex is required for ouabain-induced trafficking of NHE3. Since 100 nM ouabain had no effect on $[\text{Na}^+]_i$, it is less likely that changes in $[\text{Na}^+]_i$ are responsible for ouabain-induced trafficking of NHE3. To further investigate the effect of $[\text{Na}^+]_i$ on the ouabain-induced regulation of NHE3, an equilibrium of $[\text{Na}^+]_i$ with the extracellular Na^+ concentration was achieved using conventional “ Na^+ -clamping” methods in LLC-PK1 cells (24). LLC-PK1 cells were pretreated with either 20 μM monensin or 10 μM monensin plus 5 μM gramicidins for 30 min. Under both conditions, basal levels of NHE3 protein content in early endosomes were significantly increased, but ouabain (100 nM, 1 h) was still able to induce significant accumulation of NHE3 in early endosomes, as observed in normal control medium (Fig. 5). Again, under the same Na^+ -clamping conditions, ouabain also accumulated the $\text{Na}^+\text{-K}^+\text{-ATPase}$ α_1 -subunit in the same early endosome fraction (data not shown). These observations indicate that ouabain-induced trafficking of both NHE3 and $\text{Na}^+\text{-K}^+\text{-ATPase}$ is independent of $[\text{Na}^+]_i$.

In LLC-PK1 cells, ouabain triggers signaling cascades involving the activation of c-Src kinase and phosphatidylinositol 3-kinase (PI3K), through the caveolar $\text{Na}^+\text{-K}^+\text{-ATPase}/\text{Src}$ signaling complex. These cascades are critical in ouabain-induced endocytosis of $\text{Na}^+\text{-K}^+\text{-ATPase}$ and transcriptional regulation of NHE3 (33, 34, 43). In epithelial cells, lipid rafts and/or caveolae appear to play important roles in the trafficking of $\text{Na}^+\text{-K}^+\text{-ATPase}$ and NHE3 (31, 34, 40). To determine the role of caveolae and/or lipid rafts in the ouabain-induced trafficking of $\text{Na}^+\text{-K}^+\text{-ATPase}$ and NHE3, caveolae and/or lipid rafts were disrupted and reestablished by cholesterol depletion (using M β -CD) and repletion. Disruption of caveolae and/or lipid rafts by cholesterol depletion prevented the ouabain-induced accumulation of NHE3 in early endosomes,

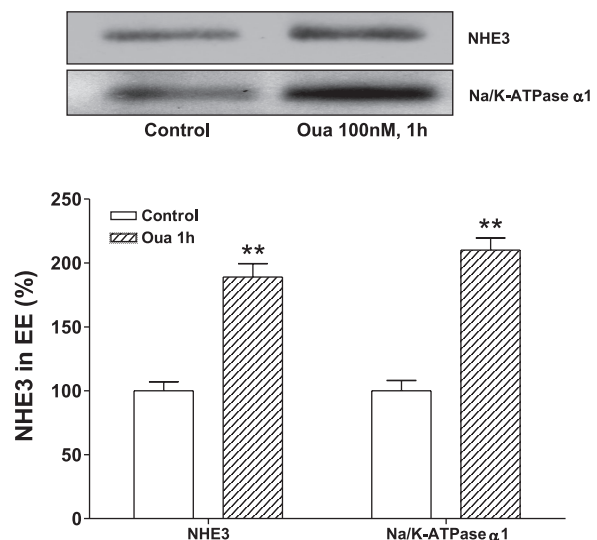


Fig. 4. Ouabain accumulates NHE3 in early endosomes (EEs) but not in late endosomes (LEs). LLC-PK1 cells were treated with or without 100 nM ouabain for 1 h. EE and LE were isolated and identified as described in MATERIALS AND METHODS. The abundance of NHE3 and the $\text{Na}^+\text{-K}^+\text{-ATPase}$ α_1 -subunit was detected by Western blot. No detectable NHE3 protein was observed in LEs. The $\text{Na}^+\text{-K}^+\text{-ATPase}$ α_1 -subunit also accumulated in LEs (data not shown). Values are means \pm SE and are expressed relative to the control. ** $P < 0.01$, ouabain treatment vs. control ($n = 9$).

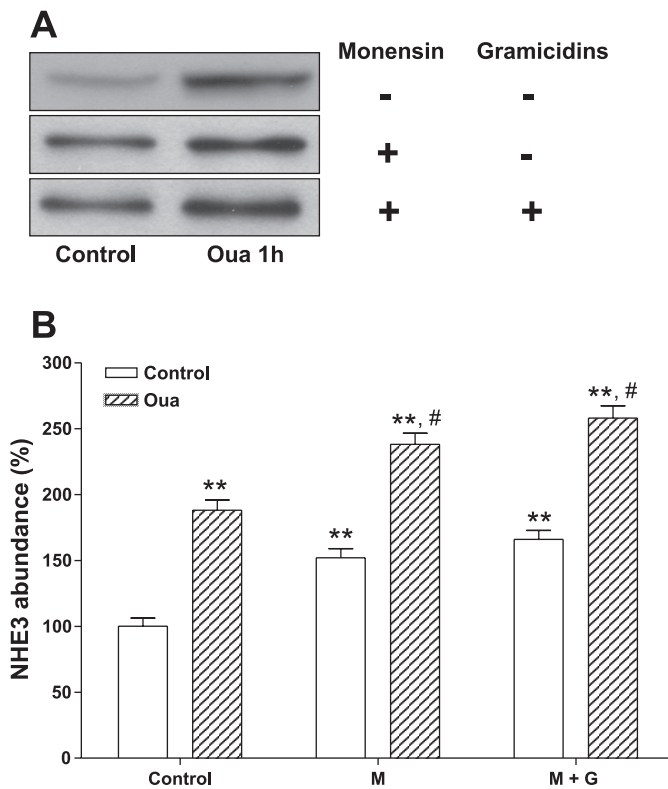


Fig. 5. Ouabain-induced endocytosis of $\text{Na}^+\text{-K}^+\text{-ATPase}$ and NHE3 is independent of $[\text{Na}^+]_i$. LLC-PK1 cells were pretreated with either 20 μM monensin (M) or 10 μM monensin plus 5 μM gramicidins (M + G) for 30 min to equilibrate $[\text{Na}^+]_i$ with the extracellular Na^+ concentration. LLC-PK1 cells in normal medium were used as controls. Cells were then treated with or without 100 nM ouabain for 1 h. The abundance of NHE3 in EEs is shown. A: representative Western blot; B: bar graph summary of the immunoblotting data. Similar results were also observed for the $\text{Na}^+\text{-K}^+\text{-ATPase}$ α_1 -subunit (data not shown). Values are means \pm SE and are expressed relative to the control in normal medium. ** $P < 0.01$, ouabain treatment vs. control; # $P < 0.01$, ouabain treatment vs. control with monensin or monensin plus gramicidins ($n = 4$).

and cholesterol repletion restored the endosomal accumulation of NHE3 (Fig. 6). Under the same conditions, the ouabain-induced accumulation of $\text{Na}^+\text{-K}^+\text{-ATPase}$ was also prevented by cholesterol depletion and restored by repletion (data not shown and Ref. 34). Moreover, M β -CD pretreatment also significantly prevented the effect of ouabain on NHE3-mediated H^+ -driven $^{22}\text{Na}^+$ uptake (data not shown). To determine the effects of Src kinase and/or PI3K, LLC-PK1 cells were preincubated with a specific inhibitor of c-Src (1 μM PP2) or PI3K (100 nM wortmannin) for 30 min and then treated with ouabain (100 nM, 1 h) in the presence of the inhibitor. Inhibition of c-Src or PI3K prevented not only the ouabain-induced downregulation of NHE3 activity (H^+ -driven $^{22}\text{Na}^+$ uptake; Fig. 7A) but also ouabain-induced NHE3 trafficking (determined by cell surface biotinylation; Fig. 7B). PP2 or wortmannin alone did not show any effect. These observations indicate that ouabain-mediated NHE3 regulation is triggered by the ouabain-activated basolateral $\text{Na}^+\text{-K}^+\text{-ATPase}/\text{Src}$ receptor complex.

Intracellular Ca^{2+} is a potential "second messenger" in the ouabain-induced regulation of NHE3. Since ouabain inhibits transepithelial Na^+ transport via a simultaneous regulation of

the two transporters without changing $[\text{Na}^+]_i$, ouabain-activated basolateral signaling has to be "moved" from the basolateral aspect to the apical aspect. Ca^{2+} signaling is involved in the control of Na^+ handling in renal epithelial cells. Binding of ouabain to $\text{Na}^+\text{-K}^+\text{-ATPase}$ has been shown to activate a $[\text{Ca}^{2+}]_i$ oscillatory signaling pathway in epithelial cells that is independent of changes in $[\text{Na}^+]_i$ (1). These findings led to the speculation that Ca^{2+} signaling may be important in the ouabain-induced regulation of NHE3. Indeed, we observed that ouabain (100 nM) significantly increased $[\text{Ca}^{2+}]_i$ in LLC-PK1 cells in normal culture medium ($\text{Ca}^{2+} = 1 \text{ mM}$), from 112.5 ± 18.9 to $236.6 \pm 21.8 \text{ nM}$ ($n = 12$, $P < 0.01$), within 15 min. Pretreatment of LLC-PK1 cells with 10 μM BAPTA-AM, a membrane-permeable Ca^{2+} chelator, did not change basal $[\text{Ca}^{2+}]_i$ levels but attenuated ouabain-induced increases in $[\text{Ca}^{2+}]_i$ ($131 \pm 16.9\%$ with BAPTA-AM vs. $210 \pm 18.8\%$ in control, $n = 9$, $P < 0.01$). Consequently, it also attenuated ouabain-induced cell surface depletion and endosomal accumulation of NHE3 (Fig. 8). This supports the notion that ouabain-activated Ca^{2+} signaling may be a potential second messenger in the ouabain-induced regulation of NHE3.

DISCUSSION

In the renal proximal tubular cell, NHE3 is expressed in the apical membrane, playing a pivotal role in transepithelial Na^+ reabsorption (2, 7, 47). $\text{Na}^+\text{-K}^+\text{-ATPase}$ resides at the basolateral surface, providing the driving force for the active vectorial transport of Na^+ from the tubular lumen to the vascular compartment. In addition to ion pumping, $\text{Na}^+\text{-K}^+\text{-ATPase}$ also functions as a receptor and signal transducer (52). Although $\text{Na}^+\text{-K}^+\text{-ATPase}$ itself lacks tyrosine kinase activity, $\text{Na}^+\text{-K}^+\text{-ATPase}$ and Src assemble into a functional receptor complex in the caveolae microdomain, which is capable of converting the extracellular ouabain signal to the activation of various signaling cascades (49, 50). As part of this $\text{Na}^+\text{-K}^+\text{-ATPase}$ signaling process, ouabain also induces clathrin-dependent endocytosis of $\text{Na}^+\text{-K}^+\text{-ATPase}$. This process requires caveolin-1 and the activation of c-Src kinase and PI3K (33, 34). In renal epithelial cells, low concentrations of ouabain

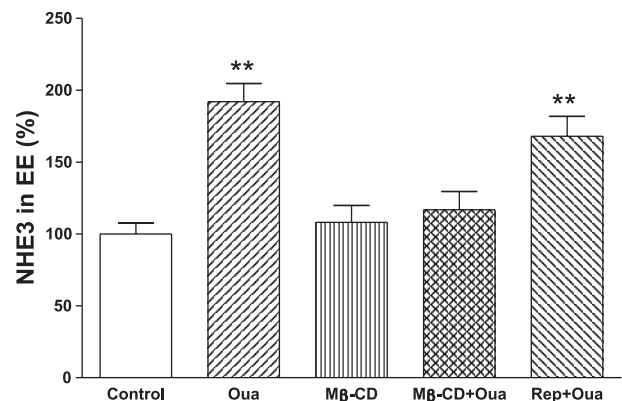


Fig. 6. Depletion of cholesterol prevents the ouabain-induced accumulation of NHE3 in EEs. Cholesterol depletion [using methyl- β -cyclodextrin (M β -CD)] and repletion (Rep) were performed as described in MATERIALS AND METHODS. After cholesterol depletion and repletion, LLC-PK1 cells were treated with ouabain (100 nM) for 1 h, and EEs were isolated. The abundance of NHE3 was determined by Western blot. Values are means \pm SE and are expressed relative to the control. ** $P < 0.01$ ouabain treatment vs. control ($n = 4$).

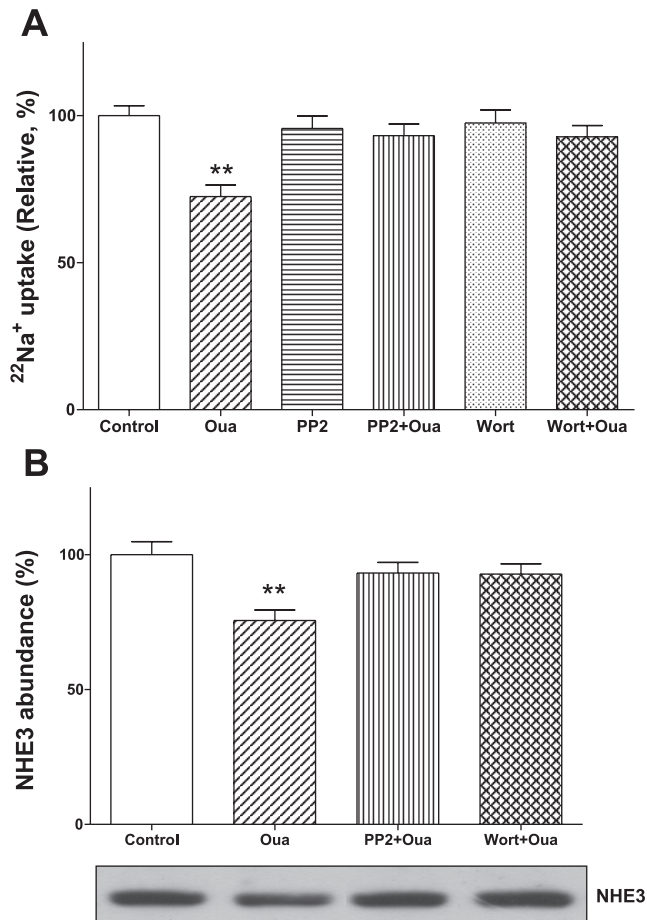


Fig. 7. c-Src and phosphatidylinositol 3-kinase (PI3K) are involved in the ouabain-induced NHE3 endocytosis and inhibition of NHE3 activity. LLC-PK1 cells were pretreated with a c-Src specific inhibitor (PP2; 1 μM , 30 min) or the PI3K-specific inhibitor wortmannin (Wort; 100 nM, 30 min) followed by ouabain treatment (100 nM, 1 h) in the continued presence of the respective inhibitor. *A*: H^+ -driven $^{22}\text{Na}^+$ uptake in response to ouabain and inhibitors ($n = 4$). *B*: abundance of cell surface NHE3 in response to ouabain and inhibitors ($n = 4$). Values are means \pm SE and are expressed relative to the control. $**P < 0.01$, ouabain treatment vs. control.

chronically reduce transepithelial Na^+ transport without a concomitant rise in $[\text{Na}^+]_i$ (43). While our initial investigations of this phenomenon demonstrated that ouabain-activated Na^+ - K^+ -ATPase/Src signaling led to the transcriptional downregulation of NHE3, we could not exclude a possible acute effect on NHE3 activity that would be necessary to effect acute changes in transepithelial Na^+ transport. The present study aimed to examine whether such acute effects could be demonstrated.

Our results suggest that acute exposure of LLC-PK1 cells to ouabain significantly inhibited transepithelial Na^+ transport by simultaneously stimulating endocytosis of basolateral Na^+ - K^+ -ATPase and apical NHE3. This process is most likely triggered by the ouabain-activated Na^+ - K^+ -ATPase/Src receptor complex in the caveolae microdomain. Ouabain seems to have biphasic effects on NHE3 regulation; acutely it stimulates NHE3 trafficking and chronically it inhibits NHE3 expression. In both processes, ouabain-activated signaling plays a central role. First, ouabain treatment significantly reduced transepithelial Na^+ transport without altering $[\text{Na}^+]_i$. These effects were

only observed with ouabain treatment on the basolateral aspect, but not on the apical aspect, suggesting that the reduced apical Na^+ entry is triggered at the basolateral membrane. Second, equilibrium of Na^+ across the membrane by Na^+ clamping did not prevent ouabain-induced early endosomal accumulation of NHE3 and Na^+ - K^+ -ATPase. Third, the ouabain effects on NHE3 activity and transepithelial Na^+ transport were blocked by c-Src and PI3K inhibitors. Moreover, whereas caveolin-1 was required in the ouabain-induced transcriptional regulation of NHE3 and endocytosis of Na^+ - K^+ -ATPase, caveolae/lipid rafts were also involved in ouabain-induced NHE3 trafficking.

At this point, we cannot conclude if NHE3 activity is closely related to the cell surface NHE3 protein content, since NHE3 activity may also be regulated through its kinetic properties [V_{max} , K_{Na^+} , and $K_{(\text{H}^+)}$] (30, 40). Even though we demonstrated a net decrease in cell surface NHE3 with a concomitant net accumulation of NHE3 in early endosomes, it is important to note that ouabain may also affect NHE3 exocytosis or recycling in this phenomenon. Since the isolated early endosomes may also contain recycling vesicles, accumulation of NHE3 in the early endosomal vesicles cannot be used as the only evidence for increased endocytosis. These issues remain to be resolved experimentally. We also noted that, in response to acute hypertension and parathyroid hormone treatment, NHE3 was redistributed to the base of microvilli but not to endosomes in the rat proximal tubule (53); however, cultured proximal tubule-derived cell lines lack microvilli and the intermicrovillar cleft structures found in the brush border of proximal tubules in situ (37). This may account for the differences observed in cultured cells.

It is well documented that ouabain-activated Ca^{2+} signaling pathways are independent of $[\text{Na}^+]_i$ changes. In cells expressing Na^+ - K^+ -ATPase α_2/α_3 -subunits, ouabain induces Ca^{2+} transients without the induction of bulk changes in $[\text{Na}^+]_i$ or modulates local increases in $[\text{Na}^+]_i$ and $[\text{Ca}^{2+}]_i$ via store-operated Ca^{2+} channels and the Na^+ / Ca^{2+} exchanger (4, 5). In cells expressing only the Na^+ - K^+ -ATPase α_1 -subunit, like LLC-PK1 cells and other kidney cells, ouabain-induced Ca^{2+} oscillation signaling is also independent of $[\text{Na}^+]_i$ (1, 39).

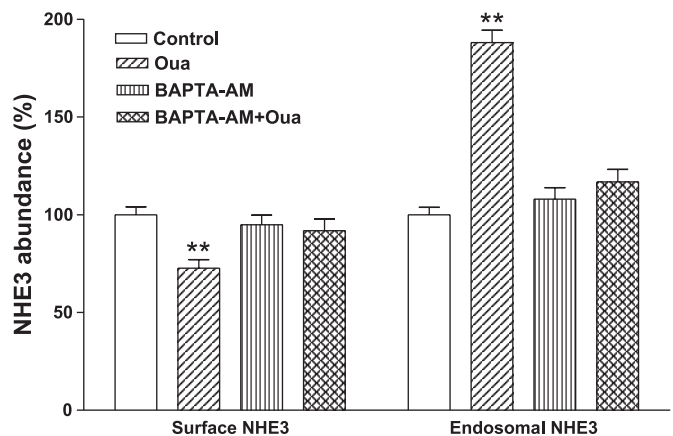


Fig. 8. Involvement of intracellular Ca^{2+} in ouabain-induced NHE3 endocytosis. LLC-PK1 cells were pretreated with 10 μM BAPTA-AM for 30 min and then treated with or without 100 nM ouabain for 1 h. Surface NHE3 was detected by surface biotinylation, and early endosomal NHE3 was detected by endosome isolation following Western blot analysis. Values are means \pm SE and are expressed relative to the control treatment. $**P < 0.01$, ouabain treatment vs. control ($n = 4$).

These data indicate that ouabain may function differently depending on the cell type and isoform. Interestingly, the binding of ouabain to Na⁺-K⁺-ATPase not only tethers PLC- γ_1 and the inositol 1,4,5-trisphosphate receptor (IP₃R) together to form a Ca²⁺-regulatory complex (54) but also stimulates the interaction of the NH₂ terminus of the endoplasmic reticulum-localized IP₃R with the NH₂ terminus of the Na⁺-K⁺-ATPase α -subunit (55). These observations support the notion that ouabain-activated Na⁺-K⁺-ATPase signaling may also regulate NHE3 in the renal proximal tubule, since intracellular Ca²⁺ has been shown to regulate NHE3 activity and trafficking (16, 29).

Our observations also raise an interesting question: how does ouabain-activated basolateral Na⁺-K⁺-ATPase/Src signaling regulate apical NHE3? Except for the role in Ca²⁺ signaling, it is reasonable to propose that ouabain-activated Na⁺-K⁺-ATPase signaling or endocytosed ouabain-Na⁺-K⁺-ATPase might serve as a "coupling point" in the regulation of transepithelial Na⁺ transport (32). Receptor-mediated endocytosis has been shown not only to attenuate ligand-activated signaling but also to continue the signaling on the endocytic pathway, especially from endosomes (38, 48). Endocytic receptor tyrosine kinase (RTK) receptors could control the magnitude of the original signaling response (generated at the cell surface) or initiate distinct signaling cascades (qualitatively different from that generated at the cell surface) (51). In polarized epithelial cells, distribution of RTK substrates could affect cellular responses (28). The endosomal signaling appears to be dependent on both the receptor and cell type. In LLC-PK1 cells, ouabain not only induced compartmentalization of Na⁺-K⁺-ATPase, c-Src, EGF receptor, and ERK in early endosomes (33) but also bound to Na⁺-K⁺-ATPase along the endocytic route (12, 35). Interestingly, caveolin-1 is also present in early or recycling endosomes. These facts make it possible that endosomal ouabain-Na⁺-K⁺-ATPase might be able to propagate its original signaling or to initiate distinct signaling cascades. This is supported by our findings that ouabain-induced NHE3 regulation is mediated by the activation of the receptor function of Na⁺-K⁺-ATPase. Furthermore, endocytosis is required for ouabain to remove basolateral Na⁺-K⁺-ATPase, which induces significant inhibition of the pumping activity. Moreover, blockade of Na⁺-K⁺-ATPase endocytosis appears to be sufficient to abolish ouabain-induced trafficking and transcriptional regulation of NHE3.

Although more work will be required to delineate the mechanism (like the role of NHE regulatory factor, NHE3 phosphorylation, and Ca²⁺ signaling), the data presented here provides new evidence for the cardiotoxic steroid-mediated regulation of transepithelial Na⁺ transport in the renal proximal tubule. This may represent an underlying mechanism of cardiotoxic steroid-mediated renal adaptation to volume expansion and/or hypertension. In this process, it is logical to propose that ouabain-activated Na⁺-K⁺-ATPase signaling (from the cell surface and/or endosomes) may regulate Na⁺ handling via synchronous regulation of both basal and apical ion transporters, but the role of endocytic ouabain-Na⁺-K⁺-ATPase and Ca²⁺ signaling in ouabain-induced NHE3 regulation remains unresolved.

ACKNOWLEDGMENTS

We are grateful to Carol Woods for the excellent secretarial assistance.

GRANTS

Portions of this work were supported by National Institutes of Health Grants HL-67963 and GM-78565 and by American Heart Association Ohio Valley Affiliate.

REFERENCES

1. Aizman O, Uhlen P, Lal M, Brismar H, Aperia A. Ouabain, a steroid hormone that signals with slow calcium oscillations. *Proc Natl Acad Sci USA* 98: 13420–13424, 2001.
2. Amemiya M, Loffing J, Lotscher M, Kaissling B, Alpern RJ, Moe OW. Expression of NHE-3 in the apical membrane of rat renal proximal tubule and thick ascending limb. *Kidney Int* 48: 1206–1215, 1995.
3. Amlal H, Chen Q, Greeley T, Pavelic L, Soleimani M. Coordinated down-regulation of NBC-1 and NHE-3 in sodium and bicarbonate loading. *Kidney Int* 60: 1824–1836, 2001.
4. Arnon A, Hamlyn JM, Blaustein MP. Na⁺ entry via store-operated channels modulates Ca²⁺ signaling in arterial myocytes. *Am J Physiol Cell Physiol* 278: C163–C173, 2000.
5. Arnon A, Hamlyn JM, Blaustein MP. Ouabain augments Ca²⁺ transients in arterial smooth muscle without raising cytosolic Na⁺. *Am J Physiol Heart Circ Physiol* 279: H679–H691, 2000.
6. Biagi B, Kubota T, Sohtell M, Giebisch G. Intracellular potentials in rabbit proximal tubules perfused in vitro. *Am J Physiol Renal Fluid Electrolyte Physiol* 240: F200–F210, 1981.
7. Biemesderfer D, Pizzonia J, Abu-Alfa A, Exner M, Reilly R, Igarashi P, Aronson PS. NHE3: a Na⁺/H⁺ exchanger isoform of renal brush border. *Am J Physiol Renal Fluid Electrolyte Physiol* 265: F736–F742, 1993.
8. Blaustein MP. Sodium ions, calcium ions, blood pressure regulation, and hypertension: a reassessment and a hypothesis. *Am J Physiol Cell Physiol* 232: C165–C173, 1977.
9. Chibalin AV, Ogomoto G, Pedemonte CH, Pressley TA, Katz AI, Feraille E, Berggren PO, Bertorello AM. Dopamine-induced endocytosis of Na⁺,K⁺-ATPase is initiated by phosphorylation of Ser-18 in the rat alpha subunit and is responsible for the decreased activity in epithelial cells. *J Biol Chem* 274: 1920–1927, 1999.
10. Chow CW, Khurana S, Woodside M, Grinstein S, Orlowski J. The epithelial Na⁺/H⁺ exchanger, NHE3, is internalized through a clathrin-mediated pathway. *J Biol Chem* 274: 37551–37558, 1999.
11. Collazo R, Fan L, Hu MC, Zhao H, Wiederkehr MR, Moe OW. Acute regulation of Na⁺/H⁺ exchanger NHE3 by parathyroid hormone via NHE3 phosphorylation and dynamin-dependent endocytosis. *J Biol Chem* 275: 31601–31608, 2000.
12. Cook JS, Tate EH, Shaffer C. Uptake of [³H]ouabain from the cell surface into the lysosomal compartment of HeLa cells. *J Cell Physiol* 110: 84–92, 1982.
13. Dahl LK, Knudsen KD, Heine M, Leitel G. Effects of chronic excess salt ingestion. Genetic influence on the development of salt hypertension in parabiotic rats: evidence for a humoral factor. *J Exp Med* 126: 687–699, 1967.
14. de Wardener HE, Clarkson EM. Concept of natriuretic hormone. *Physiol Rev* 65: 658–759, 1985.
15. Di Sole F, Cerull R, Casavola V, Moe OW, Burckhardt G, Helmle-Kolb C. Molecular aspects of acute inhibition of Na⁺-H⁺ exchanger NHE3 by A₂-adenosine receptor agonists. *J Physiol* 541: 529–543, 2002.
16. Di Sole F, Cerull R, Petzke S, Casavola V, Burckhardt G, Helmle-Kolb C. Bimodal acute Effects of A₁ adenosine receptor activation on Na⁺/H⁺ exchanger 3 in opossum kidney cells. *J Am Soc Nephrol* 14: 1720–1730, 2003.
17. Diarra ASC, Church J. In situ calibration and [H⁺] sensitivity of the fluorescent Na⁺ indicator SBFI. *Am J Physiol Cell Physiol* 280: C1623–C1633, 2001.
18. Dostanic-Larson I, Van Huysse JW, Lorenz JN, Lingrel JB. The highly conserved cardiac glycoside binding site of Na,K-ATPase plays a role in blood pressure regulation. *Proc Natl Acad Sci USA* 102: 15845–15850, 2005.
19. Fedorova OV, Kolodkin NI, Agalakova NI, Lakatta EG, Bagrov AY. Marinobufagenin, an endogenous alpha-1 sodium pump ligand, in hypertensive Dahl salt-sensitive rats. *Hypertension* 37: 462–466, 2001.
20. Gomes P, Soares-da-Silva P. Upregulation of apical NHE3 in renal OK cells overexpressing the rodent α_1 -subunit of the Na⁺ pump. *Am J Physiol Regul Integr Comp Physiol* 290: R1142–R1150, 2006.

21. Gorvel JP, Chavrier P, Zerial M, Gruenberg J. Rab5 controls early endosome fusion in vitro. *Cell* 64: 915–925, 1991.
22. Gottardi CJ, Dunbar LA, Caplan MJ. Biotinylation and assessment of membrane polarity: caveats and methodological concerns. *Am J Physiol Renal Fluid Electrolyte Physiol* 268: F285–F295, 1995.
23. Hamlyn JM, Ringel R, Schaeffer J, Levinson PD, Hamilton BP, Kowarski AA, Blaustein MP. A circulating inhibitor of (Na⁺ + K⁺)ATPase associated with essential hypertension. *Nature* 300: 650–652, 1982.
24. Harootyanian AT, Kao JP, Eckert BK, Tsien RY. Fluorescence ratio imaging of cytosolic free Na⁺ in individual fibroblasts and lymphocytes. *J Biol Chem* 264: 19458–19467, 1989.
25. Hu MC, Fan L, Crowder LA, Karim-Jimenez Z, Murer H, Moe OW. Dopamine acutely stimulates Na⁺/H⁺ exchanger (NHE3) endocytosis via clathrin-coated vesicles: dependence on protein kinase A-mediated NHE3 phosphorylation. *J Biol Chem* 276: 26906–26915, 2001.
26. Kennedy DJ, Vetteth S, Periyasamy SM, Kanj M, Fedorova L, Khouri S, Kahaleh MB, Xie Z, Malhotra D, Kolodkin NI, Lakatta EG, Fedorova OV, Bagrov AY, Shapiro JI. Central role for the cardiotoxic steroid marinobufagenin in the pathogenesis of experimental uremic cardiomyopathy. *Hypertension* 47: 488–495, 2006.
27. Khundmiri SJ, Bertorello AM, Delamere NA, Lederer ED. Clathrin-mediated endocytosis of Na⁺/K⁺-ATPase in response to parathyroid hormone requires ERK-dependent phosphorylation of Ser-11 within the alpha1-subunit. *J Biol Chem* 279: 17418–17427, 2004.
28. Kuwada SK, Lund KA, Li XF, Clifton P, Amsler K, Opreko LK, Wiley HS. Differential signaling and regulation of apical vs. basolateral EGFR in polarized epithelial cells. *Am J Physiol Cell Physiol* 275: C1419–C1428, 1998.
29. Lee-Kwon W, Kim JH, Choi JW, Kawano K, Cha B, Dartt DA, Zoukhri D, Donowitz M. Ca²⁺-dependent inhibition of NHE3 requires PKC α which binds to E3KARP to decrease surface NHE3 containing plasma membrane complexes. *Am J Physiol Cell Physiol* 285: C1527–C1536, 2003.
30. Levine SA, Montrose MH, Tse CM, Donowitz M. Kinetics and regulation of three cloned mammalian Na⁺/H⁺ exchangers stably expressed in a fibroblast cell line. *J Biol Chem* 268: 25527–25535, 1993.
31. Li X, Galli T, Leu S, Wade JB, Weinman EJ, Leung G, Cheong A, Louvard D, Donowitz M. Na⁺-H⁺ exchanger 3 (NHE3) is present in lipid rafts in the rabbit ileal brush border: a role for rafts in trafficking and rapid stimulation of NHE3. *J Physiol* 537: 537–552, 2001.
32. Liu J. Na/K-ATPase endocytosis couples pumping and leaking activities in renal epithelial cells: a hypothesis. *Cell Mol Biol (Noisy-le-grand)* 52: 97–104, 2006.
33. Liu J, Kesiry R, Periyasamy S, Malhotra D, Xie Z, Shapiro JI. Ouabain induces endocytosis of plasmalemmal Na/K-ATPase in LLC-PK1 cells by a clathrin-dependent mechanism. *Kidney Int* 66: 227–241, 2004.
34. Liu J, Liang M, Liu L, Malhotra D, Xie Z, Shapiro JI. Ouabain-induced endocytosis of the plasmalemmal Na/K-ATPase in LLC-PK1 cells requires caveolin-1. *Kidney Int* 67: 1844–1854, 2005.
35. Liu J, Periyasamy SM, Gunning W, Fedorova OV, Bagrov AY, Malhotra D, Xie Z, Shapiro JI. Effects of cardiac glycosides on sodium pump expression and function in LLC-PK1 and MDCK cells. *Kidney Int* 62: 2118–2125, 2002.
36. Liu J, Tian J, Haas M, Shapiro JI, Askari A, Xie Z. Ouabain interaction with cardiac Na⁺/K⁺-ATPase initiates signal cascades independent of changes in intracellular Na⁺ and Ca²⁺ concentrations. *J Biol Chem* 275: 27838–27844, 2000.
37. McDonough AA, Biemesderfer D. Does membrane trafficking play a role in regulating the sodium/hydrogen exchanger isoform 3 in the proximal tubule? *Curr Opin Nephrol Hypertens* 12: 533–541, 2003.
38. McPherson PS, Kay BK, Hussain NK. Signaling on the endocytic pathway. *Traffic* 2: 375–384, 2001.
39. Miyakawa-Naito A, Uhlen P, Lal M, Aizman O, Mikoshiba K, Brismar H, Zelenin S, Aperia A. Cell signaling microdomain with Na,K-ATPase and inositol 1,4,5-trisphosphate receptor generates calcium oscillations. *J Biol Chem* 278: 50355–50361, 2003.
40. Murtazina R, Kovbasnjuk O, Donowitz M, Li X. Na⁺/H⁺ exchanger NHE3 activity and trafficking are lipid raft-dependent. *J Biol Chem* 281: 17845–17855, 2006.
41. Musgrove EAH. Measurement of intracellular pH. *Methods Cell Biol* 33: 59–69, 1990.
42. Muto S, Nemoto J, Okada K, Miyata Y, Kawakami K, Saito T, Asano Y. Intracellular Na⁺ directly modulates Na⁺/K⁺-ATPase gene expression in normal rat kidney epithelial cells. *Kidney Int* 57: 1617–1635, 2000.
43. Oweis S, Wu L, Kiela PR, Zhao H, Malhotra D, Ghishan FK, Xie Z, Shapiro JI, Liu J. Cardiac glycoside downregulates NHE3 activity and expression in LLC-PK1 cells. *Am J Physiol Renal Physiol* 290: F997–F1008, 2006.
44. Periyasamy SM, Liu J, Tanta F, Kabak B, Wakefield B, Malhotra D, Kennedy DJ, Nadoor A, Fedorova OV, Gunning W, Xie Z, Bagrov AY, Shapiro JI. Salt loading induces redistribution of the plasmalemmal Na/K-ATPase in proximal tubule cells. *Kidney Int* 67: 1868–1877, 2005.
45. Rajasekaran SA, Barwe SP, Gopal J, Ryazantsev S, Schneeberger EE, Rajasekaran AK. Na-K-ATPase regulates tight junction permeability through occludin phosphorylation in pancreatic epithelial cells. *Am J Physiol Gastrointest Liver Physiol* 292: G124–G133, 2007.
46. Schoner W. Endogenous cardiac glycosides, a new class of steroid hormones. *Eur J Biochem* 269: 2440–2448, 2002.
47. Schultheis PJ, Clarke LL, Meneton P, Miller ML, Soleimani M, Gawenis LR, Riddle TM, Duffy JJ, Doetschman T, Wang T, Giebisch G, Aronson PS, Lorenz JN, Shull GE. Renal and intestinal absorptive defects in mice lacking the NHE3 Na⁺/H⁺ exchanger. *Nat Genet* 19: 282–285, 1998.
48. Sorkin A, Von Zastrow M. Signal transduction and endocytosis: close encounters of many kinds. *Nat Rev Mol Cell Biol* 3: 600–614, 2002.
49. Tian J, Cai T, Yuan Z, Wang H, Liu L, Haas M, Maksimova E, Huang XY, Xie ZJ. Binding of Src to Na⁺/K⁺-ATPase forms a functional signaling complex. *Mol Biol Cell* 17: 317–326, 2006.
50. Wang H, Haas M, Liang M, Cai T, Tian J, Li S, Xie Z. Ouabain assembles signaling cascades through the caveolar Na⁺/K⁺-ATPase. *J Biol Chem* 279: 17250–17259, 2004.
51. Wiley HS, Burke PM. Regulation of receptor tyrosine kinase signaling by endocytic trafficking. *Traffic* 2: 12–18, 2001.
52. Xie Z, Askari A. Na⁺/K⁺-ATPase as a signal transducer. *Eur J Biochem* 269: 2434–2439, 2002.
53. Yang LE, Maunsbach AB, Leong PK, McDonough AA. Differential traffic of proximal tubule Na⁺ transporters during hypertension or PTH: NHE3 to base of microvilli vs. NaPi2 to endosomes. *Am J Physiol Renal Physiol* 287: F896–F906, 2004.
54. Yuan Z, Cai T, Tian J, Ivanov AV, Giovannucci DR, Xie Z. Na/K-ATPase tethers phospholipase C and IP₃ receptor into a calcium-regulatory complex. *Mol Biol Cell* 16: 4034–4045, 2005.
55. Zhang S, Malmersjo S, Li J, Ando H, Aizman O, Uhlen P, Mikoshiba K, Aperia A. Distinct role of the N-terminal tail of the Na,K-ATPase catalytic subunit as a signal transducer. *J Biol Chem* 281: 21954–21962, 2006.
56. Zhang Y, Mircheff AK, Hensley CB, Magyar CE, Warnock DG, Chambrey R, Yip KP, Marsh DJ, Holstein-Rathlou NH, McDonough AA. Rapid redistribution and inhibition of renal sodium transporters during acute pressure natriuresis. *Am J Physiol Renal Fluid Electrolyte Physiol* 270: F1004–F1014, 1996.